Lower Hybrid Instability Driven by a Spiraling Ion Beam*

S. Seiler and M. Yamada
Plasma Physics Laboratory, Princeton University, Princeton, New Jersey 08540

and

H. Ikezi
Bell Laboratories, Murray Hill, New Jersey 07974
(Received 1 July 1976)

A lower-hybrid instability with ion cyclotron harmonics is observed to be resonantly driven by an ion beam injected obliquely to the confining magnetic field, in agreement with a linear, warm-plasma theory. Quasilinear velocity-space diffusion of the beam is observed.

The interaction between an ion beam and a magnetized plasma is a topic of growing interest.[1] Injection of neutral beams into fusion plasmas is predicted to create unstable ion velocity distributions, especially for nontangential injection,[2] which may cause rapid velocity-space diffusion of the beam.[3] Recently many groups have reported ion-beam–excited ion cyclotron modes.[4,5] A perpendicular ion-beam–driven lower-hybrid mode has been observed[6] with unmagnetized beam and target ions ($k_y\rho_i \gg 1$, $\omega_{pi}/\omega_{ci} \approx 10^2$–$10^3$) in a nonisothermal rf discharge plasma ($T_e \gg T_i$), unlike a fusion plasma, and the observed instability was nonresonant.

The significant properties of the instability reported here are the following: (1) It occurs in a magnetized isothermal target plasma ($k_\perp\rho_i \approx 1$, $\omega_{pi}/\omega_{ci} = 2$–$30$, $T_i \simeq T_e$); (2) it occurs at the lower-hybrid frequency (ω_{LH}) and/or nearby ion cyclotron harmonics; (3) it is resonantly driven by the perpendicular velocity of the ion beam ($\omega/k \approx u_{b\perp}$, $k_z \approx 0$); and (4) it is destabilized by low beam density, $(n_b/n_t)_{\text{onset}} \lesssim 0.01$, and velocity, $(u_{b\perp}/v_i)_{\text{onset}} \approx 2$. These results are well explained by a linear electrostatic theory including a numerical analysis of a warm beam-plasma dispersion relation. Furthermore, instability-induced anomalous velocity-space diffusion of the ion beam is observed.

The experiment was performed in the thermally ionized potassium plasma of the Princeton Q-1 device ($T_e \lesssim T_{i\perp} \simeq 0.35$ eV). To create an ion beam, we divide the double-ended plasma with a negatively biased mesh (80 lines/cm, $\lambda_{\text{space}} < \lambda_{De}$) used to prevent electron flow[7,4]; and the beams are accelerated from the positively biased source side into the grounded target plasma along the normal to the mesh surface (see Fig. 1). The angle with respect to the uniform magnetic field (1–7 kG in $\hat{z}$ direction) and the energy (0–100 eV) of the beam determine its spiral radius ρ_b and pitch length L_{pitch}. Both a fixed ring of meshes, each at a 45° angle, and a 4-mm-diam circular mesh whose angle could be varied (−30° to + 30°) were used to create the beam; and Langmuir and energy analyzer probes were used to confirm its helical path. Because of end-plate sheath acceleration, the target plasma drifts at approximately the ion sound velocity and has $T_{i\parallel} < T_{i\perp}$.[4] However, because $k_z \approx 0$, the instability is independent of both the drift and the parallel ion temperature.

The identification of the instability as a lower-hybrid mode begins with the frequency measurements shown in Fig. 2, where the spectrum shifts with target density in agreement with the relation $\omega \simeq (\omega_{pi}^2 + \omega_{ci}^2)^{1/2}$ while the beam parameters are held constant. The instability occurs at just above the cyclotron harmonics near ω_{LH}, $\omega = n\omega_{ci} + \delta$, while the number of the harmonics present depends on the beam-target density ratio.

In the simple, cold, unmagnetized electron-beam–plasma interaction, the most unstable mode is near ω_{pe}.[8] For a wave propagating perpendicular to B, strongly magnetized electrons do not contribute to the wave dynamics ($\omega/k_z \gg v_e$,

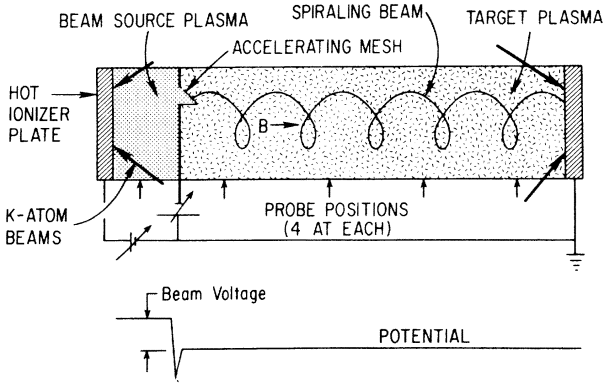

FIG. 1. Schematic of the machine layout.

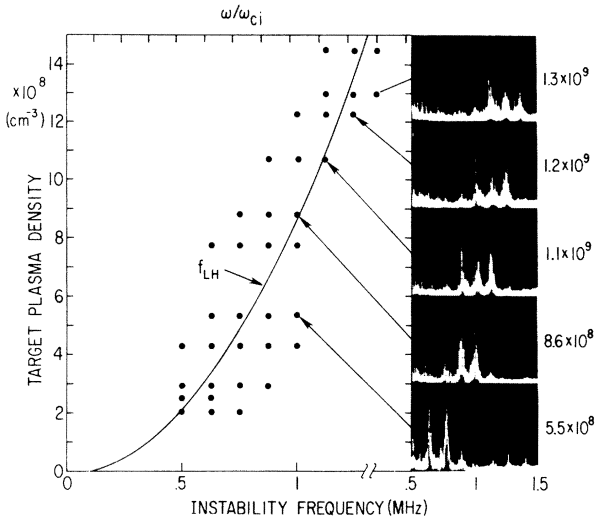

FIG. 2. Frequency shift versus the target density for constant beam energy and density. Data points are the peak frequencies of the harmonics present at each density. The solid line is $f_{LH}=(\omega_{pi}^2+\omega_{ci}^2)^{1/2}/2\pi$. Frequency spectra are shown at selected densities.

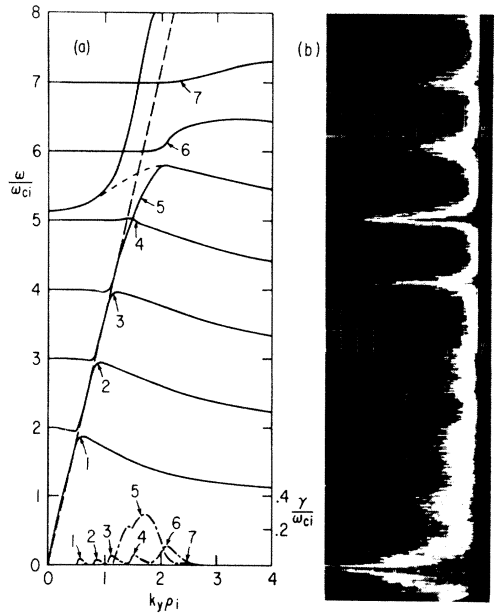

FIG. 3. Dispersion relation and spectrum. (a) Computed for $n_t=5.5\times10^8$ cm^{-3}, $n_b=4\times10^6$ cm^{-3}, $T_t=0.35$ eV, $B=4$ kG, $u_{b\perp}=3.6v_i$, $f_{LH}=5.1f_{ci}$. The dashed line indicates beam velocity ($u_{b\perp}=\omega/k_y$); the dot-dashed, the growth rates corresponding to the different cyclotron harmonics. (b) Observed frequency spectrum with the same parameters.

$k_y\rho_e\ll1$, $\omega_{pe}/\omega_{ce}\ll1$), so that an ion beam perpendicular to a magnetically confined target plasma can easily excite perpendicularly propagating ion Bernstein waves[9] at $\omega\approx n\omega_{ci}$, and the most unstable mode is near ω_{pi}.[10]

The linear, electrostatic theory presented here uses a slab model with warm, Maxwellian beam and target ions and includes the kinetic coupling. The target ions are magnetized with $k_y\rho_i\approx1$ and temperature $T_t=T_{i\perp}$, but the perpendicularly injected beam ions are treated as unmagnetized, with velocity $u_{b\perp}$ and thermal velocity spread $v_b\ll u_{b\perp}$. Collisions are negligible since for the plasma conditions used $\lambda_{mfp}\gg L_{machine}$. The dispersion relation for $k_z\approx0$, $\omega_{pe}/\omega_{ce}\ll1$, is

$$0=1-\frac{k_{Di}^2}{k^2}\left[2e^{-\lambda}\sum_{n=1}^{\infty}\frac{(n\omega_{ci})^2}{\omega^2-(n\omega_{ci})^2}I_n(\lambda)+\frac{1}{2}\frac{n_b}{n_t}\frac{T_t}{T_b}Z'\left(\frac{\omega-ku_{b\perp}}{kv_b}\right)\right], \quad (1)$$

where $\lambda=k_y^2\rho_{it}^2/2$, $\rho_{it}=(2T_t/M\omega_{ci}^2)^{1/2}$, $k_{Di}^2=4\pi n_te^2/T_t$, $v_{i(b)}=(2T_{i(b)}/M)^{1/2}$, $u_{b\perp}$ is the beam perpendicular velocity, $n_{t(b)}$ is the target (beam) density, I_n is the modified Bessel function of nth order, and Z' is the derivative of plasma dispersion function.

This equation is mathematically similar to the one used for electron Bernstein waves driven by a perpendicular ion beam,[11] and was solved numerically using experimentally measured parameter values. Without the beam term it is the ion Bernstein dispersion relation.[9] Figure 3(a) shows the calculated dispersion curve for the beam-plasma system when the spectrum of Fig. 3(b) was taken. The coupling between the beam acoustic mode and the target ion Bernstein waves is clearly seen and the maximum growth is near the lower-hybrid frequency in agreement with the experiment. In Fig. 3(b), the peak below ω_{ci} is a mode driven by the beam's parallel velocity component.[4]

This instability is resonant with the beam's perpendicular velocity and propagates azimuthally for all angles of injection. The resonance is confirmed in Fig. 4, where 4(a) shows the variation of the phase velocity ω/k of a single mode with $u_{b\perp}$ and 4(b) the phase velocities of many cyclotron modes occurring for a single beam velocity. Some spread in the angle of injection is caused by the finite ratio of Debye length to mesh spacing[12] and may explain the spread of phase velocities in Fig. 4(a). Mode selection due to the closed azimuthal propagation ($m\lambda_y=2\pi\rho_b$, where m is the azimuthal mode number) was observed and used to measure the group velocity, $d\omega/dk\approx\Delta\omega\rho_b/(M_1-M_2)$, around the most unstable harmonic; the results were in agreement with theory.

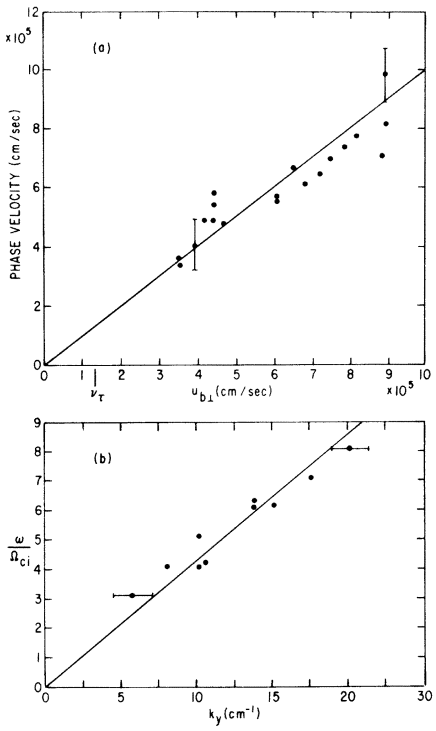

FIG. 4. Beam-wave resonance. (a) Perpendicular phase velocity of a single mode versus the perpendicular beam velocity. (b) Dispersion for harmonics for a single beam energy. The solid line indicates a constant phase velocity.

Phase shift measurements indicate that the instability is a standing wave both in the parallel direction[13] with $\lambda_z \gtrsim 2L_{\text{machine}} \gg L_{\text{pitch}}$ and in the radial direction with $k_x \simeq \pi/\rho_b < k_y$. Since perpendicularly propagating waves are not subject to either Landau or ion cyclotron damping, instability onset in this experiment is determined by the requirement that $\tau_{\text{conf}}\text{Im}\omega > 1$, where τ_{conf} is the beam lifetime[13] ($\approx 100/\omega_{ci}$). Because of its closed azimuthal propagation and standing wave parallel nature, the instability has no spatial growth. Temporal growth rates exceeding ω_{ci} are predicted by Eq. (1) for $n_b \gtrsim 0.05 n_t$ and $u_{b\perp}/v_i \gtrsim 3.5$, but since the beam transit time in the linear machine is much longer than the growth time and the parallel wavelength is longer than the machine, no reliable growth rate measurements could be obtained with pulsed beams. It is noteworthy, however, that the spectra observed in the nonlinear, saturated state exhibited maxima at the most unstable frequencies of the linear calculations, indicating the absence of strong mode-mode coupling or cascading phenomena.[14] The saturated amplitudes observed were roughly proportional to the linearly calculated growth rates. As n_b/n_t is increased from 0.01 (slightly above onset) to 0.1, the peak rms instability amplitude increases from $\tilde{n}/n_t \approx 0.005$ to 0.06. The measured dependences of onset and amplitude on the beam and target parameters were in qualitative agreement with the theory even when the unmagnetized beam approximation should break down at low beam energy.

By using an ion energy analyzer, the positive slope of the beam's perpendicular velocity distribution was observed to be flattened by nonlinear wave-particle interactions when a strong instability was present. An estimate of the time necessary for perpendicular velocity-space diffusion can be made from quasilinear theory[3]; using the experimental parameters it is $\tau_0 \approx 7/\omega_{ci} \ll \tau_{\text{conf}}$ and the identification of the flattening as quasilinear velocity-space diffusion is therefore justified. Anomalous heating of the target plasma could not be detected and was not expected because of the absence of electron Landau and ion cyclotron damping.

We have observed a lower-hybrid instability driven by a perpendicular ion beam and instability-induced nonlinear beam slowing. Good agreement was found with a warm-plasma theory. This mode required much less beam density for destabilization than the parallel ion-beam–driven ion cyclotron modes,[4] and thus has stronger impact on neutral beam injection into fusion machines in which $n_b/n_t \ll 1$. Similar ion distributions to the one in the present experiment can occur in both tokamaks and mirror machines during perpendicular neutral beam injection and anomalous velocity-space diffusion is expected to play a major role in beam slowing,[2] and in plasma confinement in mirror machines.[15] In the preheating stage this anomalous effect may be useful but it will have deleterious effects on the deuteron injection-burning stage because of the anomalous loss of fusable ions.

It is a pleasure to thank Dr. F. W. Perkins, Dr. T. H. Stix, Dr. H. P. Eubank, and Dr. R. M. Kulsrud for their valuable discussions and comments.

*This work was supported by U. S. Energy Research and Development Administration, Contract No. E(11-1)-3073, and H. Ikezi's work by Bell Laboratories.

[1]H. L. Berk *et al.*, Nucl. Fusion 15, 819 (1975); T. Stix, Phys. Fluids 16, 1922 (1973); B. Coppi and D. K. Bhadra, Phys. Fluids 18, 692 (1975).

[2]J. G. Cordey and M. J. Houghton, Nucl. Fusion 13, 215 (1973).

[3]V. M. Kulygin *et al.*, Plasma Phys. 13, 1111 (1971).
[4]H. Hendel *et al.*, Phys. Rev. Lett. 36, 319 (1976).
[5]R. P. H. Chang and M. Porkolab, Nucl. Fusion 16, 142 (1976); P. Michelsen *et al.*, Phys. Fluids 19, 453 (1976); H. Böhmer *et al.*, Phys. Fluids 19, 450 (1976); A. P. H. Goede *et al.*, Nucl. Fusion 16, 85 (1976).
[6]R. P. H. Chang, Phys. Rev. Lett. 35, 285 (1975).
[7]T. J. Taylor *et al.*, Rev. Sci. Instrum. 43, 1675 (1972).
[8]R. J. Briggs, *Electron-Stream Interaction with Plasmas* (MIT, Cambridge, Mass., 1964).
[9]I. B. Bernstein, Phys. Rev. 109, 10 (1958); J. P. M. Schmitt, Phys. Rev. Lett. 31, 982 (1973).
[10]J. B. McBride *et al.*, Phys. Fluids 15, 2367 (1972).
[11]D. W. Forslund *et al.*, Phys. Rev. Lett. 25, 1266 (1970).
[12]R. W. Motley, *Q Machines* (Academic, New York, 1975).
[13]F. F. Chen, Plasma Phys. 7, 399 (1965).
[14]T. M. Dupree, Phys. Fluids 11, 2680 (1968).
[15]D. E. Baldwin *et al.*, Phys. Rev. Lett. 36, 1051 (1976).

Neutron Emission from a Turbulently Heated High-Voltage Theta-Pinch Plasma*

Y. G. Chen
Department of Physics and Astronomy, University of Maryland, College Park, Maryland 20742
(Received 5 April 1976)

Spatial and temporal origins of three distinct neutron emission peaks observed in the University of Maryland turbulently heated high-voltage theta pinch machine have been identified. They are the result of fusion reactions involving reflected hot deuterium ions, pinched plasma, and energetic ions colliding with deuterium absorbed on the vacuum vessel wall, respectively. Studies of the wall-interaction neutron peak further reveal that the particle end loss in the reversed-field case is substantially slower than in the parallel-field case.

Neutron yields have been used as a diagnostic to measure the plasma temperatures in theta-pinch experiments by assuming that the plasma is Maxwellian and that the neutrons originate from the bulk of the compressed plasma. The time development of neutron emission observed by fast scintillators agrees well with the pinch dynamics.[1] Because of the unique feature of the University of Maryland high-voltage theta pinch machine (the coil is immersed in a water tank for field grading) we are able to construct directional neutron detectors of a limited acceptance solid angle. We therefore can distinguish both the spatial and temporal origins of the neutrons. In this Letter I report that in addition to the main neutron pulse, which does coincide in time with the plasma pinching to the axis, two more distinct neutron pulses have been observed, one before and the other after the main pulse. Figure 1 shows a cross-sectional view of the University of Maryland high-voltage theta pinch machine; a fast liquid scintillator (NE213), 5 cm in diameter and thickness, in conjunction with a RCA8575 photomultiplier, is carefully shielded electromagnetically, and totally enclosed in a heavy lead housing (~2 cm thickness). This neutron detector as shown in top center of Fig. 1 is kept in a water-tight plastic cylinder. The surrounding water serves to moderate and absorb lateral neutrons. It limits the detection solid angle to the photomultiplier tube axial direction which is perpendicular to the pinched plasma column. A cadmium sheet with a large thermal-neutron absorption coefficient has been wrapped around the scintillator laterally to improve its directivity. The detector can be moved freely upward with respect to the plastic housing to further increase the directivity. The water-tight plastic housing and detector can be moved axially (z direction) to sit on top of the pinch coil to detect neutrons from plasma within the coil or anywhere on top of the glass vacuum vessel outside of the pinch coil to detect the neutrons from

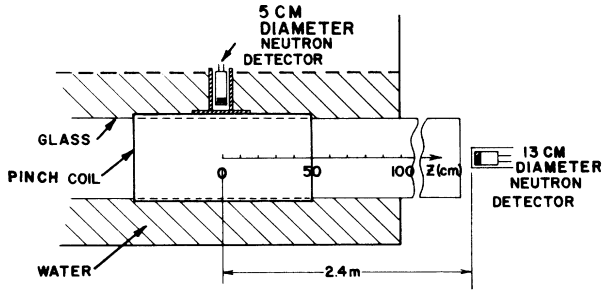

FIG. 1. A cross-sectional view of the 1-m-long, 45-cm-i.d., theta-pinch coil, water tank, and neutron detectors.

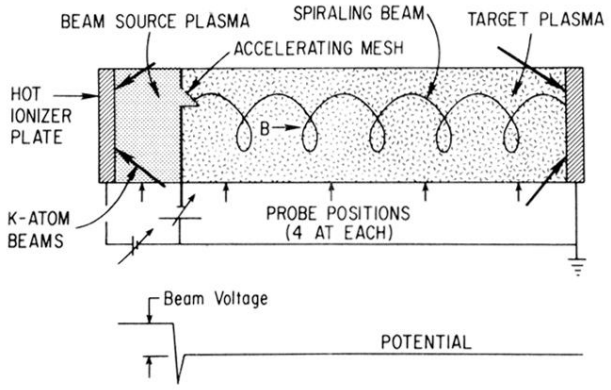

FIG. 1. Schematic of the machine layout.

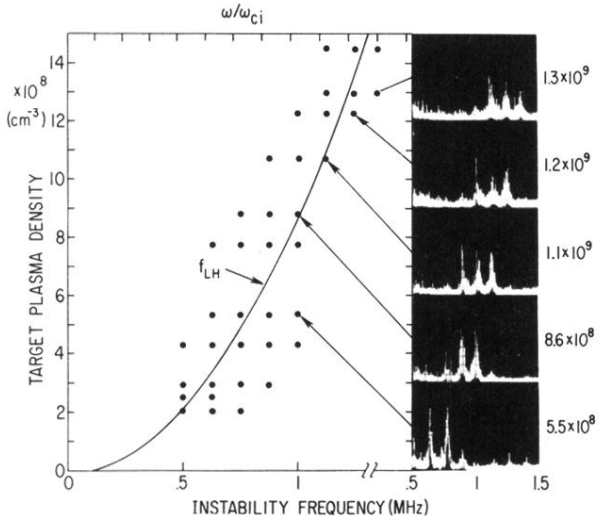

FIG. 2. Frequency shift versus the target density for constant beam energy and density. Data points are the peak frequencies of the harmonics present at each density. The solid line is $f_{LH} = (\omega_{pi}^2 + \omega_{ci}^2)^{1/2}/2\pi$. Frequency spectra are shown at selected densities.

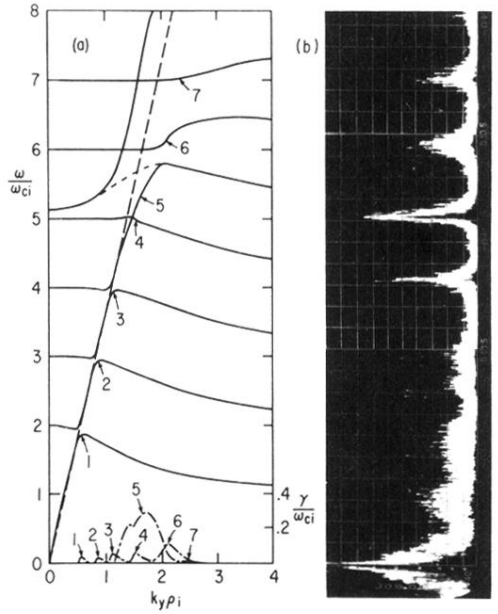

FIG. 3. Dispersion relation and spectrum. (a) Computed for $n_t = 5.5\times 10^8$ cm^{-3}, $n_b = 4\times 10^6$ cm^{-3}, $T_t = 0.35$ eV, $B = 4$ kG, $u_{b\perp} = 3.6v_i$, $f_{LH} = 5.1f_{ci}$. The dashed line indicates beam velocity ($u_{b\perp} = \omega/k_y$); the dot-dashed, the growth rates corresponding to the different cyclotron harmonics. (b) Observed frequency spectrum with the same parameters.